

Journal Pre-proofs

Research papers

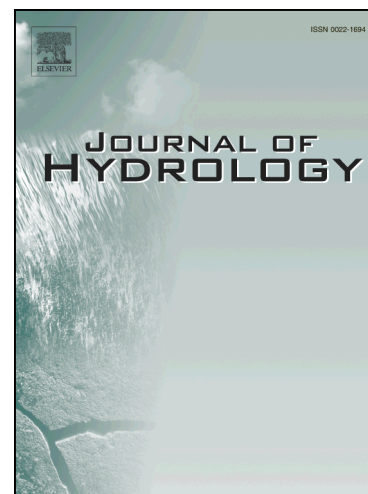
Influences of leaf area index and albedo on estimating energy fluxes with HOLAPS framework

Jian Peng, Said Kharbouche, Jan Peter-Muller, Olaf Danne, Simon Blessing, Ralf Giering, Nadine Gobron, Ralf Ludwig, Benjamin Müller, Guoyong Leng, Thomas Lees, Simon Dadson

PII: S0022-1694(19)30980-1
DOI: <https://doi.org/10.1016/j.jhydrol.2019.124245>
Reference: HYDROL 124245

To appear in: *Journal of Hydrology*

Received Date: 15 April 2019
Revised Date: 7 October 2019
Accepted Date: 15 October 2019



Please cite this article as: Peng, J., Kharbouche, S., Peter-Muller, J., Danne, O., Blessing, S., Giering, R., Gobron, N., Ludwig, R., Müller, B., Leng, G., Lees, T., Dadson, S., Influences of leaf area index and albedo on estimating energy fluxes with HOLAPS framework, *Journal of Hydrology* (2019), doi: <https://doi.org/10.1016/j.jhydrol.2019.124245>

This is a PDF file of an article that has undergone enhancements after acceptance, such as the addition of a cover page and metadata, and formatting for readability, but it is not yet the definitive version of record. This version will undergo additional copyediting, typesetting and review before it is published in its final form, but we are providing this version to give early visibility of the article. Please note that, during the production process, errors may be discovered which could affect the content, and all legal disclaimers that apply to the journal pertain.

Influences of leaf area index and albedo on estimating energy fluxes with HOLAPS framework

Jian Peng^{1,2,3*}, Said Kharbouche⁴, Jan Peter-Muller⁴, Olaf Danne⁵, Simon Blessing⁶, Ralf Giering⁶, Nadine Gobron⁷, Ralf Ludwig², Benjamin Müller², Guoyong Leng⁸, Thomas Lees¹, Simon Dadson¹

¹ School of Geography and the Environment, University of Oxford, OX1 3QY Oxford, UK;

² Department of Geography, University of Munich (LMU), 80333 Munich, Germany;

³ Max Planck Institute for Meteorology, 20146 Hamburg, Germany;

⁴ Department of Space and Climate Physics, University College London, Holmbury St Mary, UK;

⁵ Brockmann Consult GmbH, Max-Planck Str.2, 21502 Geesthacht, Germany;

⁶ FastOpt, Hamburg, Germany;

⁷ Directorate for Sustainable Resources, European Commission, Joint Research Centre, Ispra, Italy;

⁸ Environmental Change Institute, University of Oxford, OX1 3QY Oxford, UK;

* Author to whom correspondence should be addressed; E-Mail: jian.peng@ouce.ox.ac.uk;

Abstract

The High resOLution Land Atmosphere surface Parameters from Space (HOLAPS) programme provides a modeling system to maximize the use of satellite-based products and ensure internally consistent estimation of surface water and energy fluxes. Leaf area index (LAI) and land surface albedo are two key parameters for estimation of latent and sensible heat fluxes with HOLAPS. Thus, to facilitate the generation of long-term high accuracy latent and sensible heat fluxes, high quality global long-term LAI and land surface albedo datasets are essential. The Quality Assurance for Essential Climate Variables (QA4ECV) project released quality-assured long-term LAI and albedo datasets with traceable and reliable uncertainty information provided in the dataset. Taking MODIS-BNU-LAI and MODIS albedo as reference, different global long-term LAI and albedo datasets including GlobAlbedo, QA4ECV and GLOBMAP were investigated for estimation of latent/sensible heat fluxes with HOLAPS in this study. The results show that all albedo datasets show similar accuracy for estimation of latent and sensible heat fluxes when validated against FLUXNET observations. The QA4ECV LAI leads to worse latent heat flux estimation due to its use of effective LAI rather than green leaf LAI. Sensitivity analysis also shows that the HOLAPS estimated latent heat flux (LE) is more sensitive to uncertainty in LAI than land surface albedo. Overall, the combined use of QA4ECV albedo and GLOBMAP LAI is suggested for estimation of latent/sensible heat fluxes with HOLAPS. The root mean square differences (RMSD) between estimations and FLUXNET measurements are 54 (30) W/m² for hourly (monthly) latent heat flux, and 80.5 (24.5) W/m² for sensible heat flux, which are comparable to estimates with MODIS and other reported studies.

Keywords: HOLAPS, Albedo, Leaf area index, QA4ECV, MODIS, GlobAlbedo, GLOBMAP, FLUXNET

1 Introduction

Land-atmosphere interactions are crucial interface within the Earth system comprising energy and water exchange, and biogeochemical cycles (e.g. Betts et al., 1996; Suni et al., 2015). Quantification of land-atmosphere interactions is therefore extremely important for describing, understanding and predicting the Earth system (e.g. Koster et al., 2006; Seneviratne et al., 2006). Over the past few decades, significant efforts have been made to enhance our understanding of essential water and energy fluxes such as precipitation, soil moisture and evapotranspiration/latent heat flux (e.g. Milly and Shmakin, 2002; Oki and Kanae, 2006; Peng et al., 2017b; Trenberth et al., 2007). However, the quantification of global return flow of water (evapotranspiration) and energy (sensible heat flux) from land back to atmosphere is still challenging (Wang and Dickinson, 2012; Zhang et al., 2016). For example, evapotranspiration (ET) itself is a simple concept, but the complicated physical mechanisms of the ET process including turbulent transport, biophysical characteristic of transpiration, feedback within the soil-plant-atmosphere continuum and the heterogeneity of land surfaces all combine to make ET become an elusive and uncertain water and energy flux (Allen et al., 1998; Mu et al., 2011; Peng et al., 2019).

Despite these challenges, much progress has been made to measure land-atmosphere fluxes at the ecosystem scale using eddy covariance in flux tower networks (Baldocchi, 2008; Baldocchi et al., 2001), which significantly increases the availability of in-situ turbulent flux measurements over the globe. Continuous efforts have also been made to generate regional and global datasets of water and energy fluxes with satellite observations and land surface models (e.g. Courault et al., 2005; Kalma et al., 2008). Regarding ET (or latent heat flux), various methods such as energy balance models (e.g. Fisher et al., 2008; Miralles et al., 2011; Su, 2002), empirical statistical

models (e.g. Jung et al., 2011; Peng et al., 2013; Wang et al., 2007) and land surface models (e.g. Leng et al., 2013; Roads and Betts, 2000) have been proposed to make full use of satellite observations and meteorological forcing datasets. These algorithms have also led to the generation of long-term global ET datasets (e.g. Loew et al., 2016; Martens et al., 2017; Mu et al., 2007; Zhang et al., 2010). However, large discrepancies remain in these datasets due to different methods and input datasets applied to estimate ET (Jiménez et al., 2011; Mueller et al., 2013). Comprehensive evaluation studies by Miralles et al. (2016), McCabe et al. (2016), Michel et al. (2016), Richard et al. (2018) and Ershadi et al. (2014) together with Fisher et al. (2017) highlight the significance of improving the physical representation of ET. Specifically, some studies applied the same forcing datasets to investigate the differences of model assumptions (McCabe et al., 2016; Michel et al., 2016), while other studies quantified the impacts of different forcing data on the estimation of ET for the same model (Badgley et al., 2015; Vinukollu et al., 2011). The error of about 20% for global mean ET has been reported to be induced by the use of forcing data. Nevertheless, it is still challenging to attribute errors to specific model formulations or variables due to the combined effects of model parameterizations, uncertainties of forcing data, as well as error propagation within the model (Talsma et al., 2018). Compared to ET, the estimation of global sensible heat flux presents more challenges, such as parameterization of the aerodynamic resistance, and difficulties in measuring air temperature from satellite (Siemann et al., 2018). Limited long-term global sensible heat flux datasets are available based entirely on satellite observations (Vinukollu et al., 2011; Wild et al., 2015). Recently, machine learning methods have been applied to estimate global heat flux based on FLUXNET, satellite and meteorological measurements (Hobeichi et al., 2018; Jiménez et al., 2018; Yao et al., 2017). This

type of methods provides an alternative to provide global scale fluxes, however, improvement of the physical understanding and parameterization of process-based model is still essential.

To deal with the challenges of generating internally consistent, long-term and high resolution, global datasets of energy and water fluxes from satellite observations, the High resOlution Land Atmosphere surface Parameters from Space (HOLAPS) model (Loew et al., 2016) is a framework that is designed to estimate internally-consistent water and energy fluxes (particularly latent heat flux and sensible heat flux) from remote sensing observations. HOLAPS is based on a state-of-the-art land surface model. It is forced exclusively with globally available data at high temporal and spatial resolution (Loew et al., 2016; Peng et al., 2016). The key features of HOLAPS include internally consistent retrieval of longwave and shortwave radiation, and coupling with a planetary boundary layer model to constrain surface fluxes. In order to generate long-term sensible and latent fluxes datasets with HOLAPS, long-term leaf area index (LAI) and land surface albedo datasets are essential. However, there are large discrepancies in existing satellite-based LAI and albedo products and these biases might induce large uncertainties in ET estimation (Jiang et al., 2017; Song et al., 2019). A few studies have investigated how the uncertainty in LAI and albedo lead to uncertainties in model simulated carbon and water fluxes. For example, Richard et al. (2018) examined the sensitivity of gross primary productivity (GPP) and ET to satellite-derived LAI using a terrestrial biosphere model over China. They found that large discrepancies in LAI could introduce considerable uncertainties in simulated GPP and ET. A sensitivity analysis study by Kala et al. (2014) also found that model simulated heat, moisture, and carbon fluxes are sensitive to LAI. In addition, a previous study showed that errors in albedo could lead to inaccurate estimates of both evapotranspiration and sensible heat flux (Mattar et al., 2014). Therefore, the impacts of different satellite-derived LAI and albedo products on

estimation of global latent/sensible heat fluxes should be explored and determined before generation of global water and energy fluxes. The recently-completed Quality Assurance for Essential Climate Variables (QA4ECV) project released quality-assured long-term LAI and albedo datasets with traceable and reliable uncertainty information provided in the dataset (Nightingale et al., 2018; Peng et al., 2017a). QA4ECV albedo and LAI datasets provide great potential for estimating global long-term latent/sensible heat fluxes with HOLAPS. The objective of the current study is to investigate the impacts of different LAI and albedo datasets on the estimation of latent and sensible fluxes with the HOLAPS framework. A brief introduction to HOLAPS is given in section 2. The forcing datasets and flux tower measurements are introduced in section 3. The results are analyzed and discussed in section 4, with conclusion summarized in section 5.

2 Methodology

2.1 HOLAPS

HOLAPS provides a flexible framework for the generation of land surface energy and water fluxes. It is based on a land surface model and designed to maximize the use of satellite products as forcing. The combination of the planetary boundary layer (PBL) and land surface dynamics allows for a consistent simulation of the surface downwelling shortwave and longwave fluxes and enables a better constraint on land surface heat flux estimates. The core modules of HOLAPS are briefly introduced below:

Radiation module: The all sky shortwave solar surface irradiance is calculated using the MAGIC radiative transfer model (Mueller et al., 2009; Posselt et al., 2012), which requires aerosol properties, surface albedo, and total column water vapor content (TCW). For the generation of

global water and energy fluxes, the aerosol properties and the total column water vapor content can be taken from either an aerosol climatology or re-analysis data (Kinne et al., 2013). The cloud coverage is calculated by the radiation module when the radiation is provided as input. The longwave surface downwelling radiation flux is dependent on the near surface moisture (calculated within water balance model), temperature profiles and cloud coverage. It is calculated using a mixed layer model of the Planetary Boundary Layer, similar to the model developed by Margulis and Entekhabi (2001). This direct coupling of a land surface scheme with a PBL model is an obvious advantage for HOLAPS.

Land surface model: A combined model of the land surface and the PBL is used to simulate high resolution surface water and energy fluxes. Combined modelling of the PBL and land surface dynamics allows for consistent simulation of the surface downwelling shortwave and longwave fluxes as well as allows to better constrain land surface heat flux estimates. The general equation for the surface energy budget is given as:

$$R_N - LE - H - G = 0 \quad (1)$$

where R_N is the net surface radiation, LE and H are latent and sensible heat fluxes and G is the ground heat flux respectively. The net surface radiation is estimated from the sum of shortwave and longwave radiation (Liang et al., 2010):

$$R_N = (1 - \alpha)R^\downarrow + \epsilon L^\downarrow - \epsilon \sigma T_s^4 \quad (2)$$

where α is land surface albedo, R^\downarrow is shortwave downwelling radiation, ϵ is surface emissivity, L^\downarrow is longwave downwelling radiation, σ is Stefan Boltzmann constant and T_s is land surface temperature.

The surface sensible heat flux is calculated as:

$$H = \rho c_p (T_s - T_a) / r_a \quad (3)$$

where ρ is density of dry air, c_p is heat capacity of dry air, T_a is air temperature. The aerodynamic surface resistance r_a is calculated based on the Monin Obukhov similarity theory with stability correction functions after Paulson (1970). Latent heat flux is estimated based on a modified Priestley-Taylor approach (Priestley and Taylor, 1972) as:

$$LE = \phi \alpha_p R_N \frac{\Delta}{\Delta + \gamma} \quad (4)$$

where ϕ is an inhibition function, depending on temperature, radiation and soil moisture condition, α_p is Priestley-Taylor parameter for equilibrium ET and equals to 1.26, Δ is the slope of the water vapor saturation curve, and γ is the psychrometer constant.

Water balance model: The surface water balance in HOLAPS is described as the following equation:

$$P - Q - ET - \frac{\partial I}{\partial t} = \frac{\partial W}{\partial t} \quad (5)$$

where P is precipitation, Q is runoff, ET is evapotranspiration, I is water interception by the canopy and W is water storage in soil. The soil moisture dynamics is calculated using a multilayer soil scheme (0.05, 0.1, 0.25, 0.6, 1.0) m, with soil moisture fluxes between different soil layers simulated based on the Richards equation (Richards, 1931). In the current model, only the vertical soil moisture flux is considered. Once the maximum infiltration capacity is reached, the excess of water that cannot infiltrate the soil is denoted as runoff.

2.2 Sensitivity analysis

A simple sensitivity analysis study is conducted to investigate the HOLAPS's sensitivity to land surface albedo and LAI. The approach includes perturbing each variable with added uncertainty and then analyzing the model simulated LE and H in reference to the perturbation. Specifically, the HOLAPS model was forced at 48 FLUXNET stations for three years (2003-2005). The errors at six levels (1%, 5%, 10%, 20%, 30%, 40%) were added to albedo and LAI respectively. The HOLAPS simulation was then repeated at each error level and for albedo and LAI. In order to represent the model sensitivity, the relative error (RE) was calculated with:

$$R = \frac{z - y}{y} * 100\% \quad (6)$$

where y is the unperturbed estimate of LE or H, z is the perturbed estimate. After that, the sensitivity of HOLAPS to different satellite-based albedo and LAI datasets was explored. The multiple years of HOLAPS simulations were conducted with inputs mainly from FLUXNET measurements except LAI and albedo from satellite-based products. The simulated LE and H are then compared with measured quantities from FLUXNET. The results are quantified at hourly, daily and monthly timescales using standard statistical metrics including coefficient of determination (R^2), root mean square difference (RMSD) and centered root mean square difference (cRMSD) (Taylor, 2001). The above analysis aims to investigate the impacts of different LAI and albedo on the HOLAPS simulated LE and H.

3 Data

3.1 Satellite-based LAI/albedo datasets

The land surface albedo datasets used in the current study include MODIS albedo, GlobAlbedo and QA4ECV albedo. The details of these albedo datasets are briefly introduced below.

MODIS-albedo: the MODIS albedo product from early 2000 is based on clear-sky, atmospherically corrected surface reflectances that are coupled with a Bidirectional Distribution Reflectance Model (BRDF) model to establish the surface anisotropy. The product is available at spatial resolution of 500 m and 0.05° , and has already been extensively validated against ground-based measurements by many studies (Cescatti et al., 2012; Stroeve et al., 2005). The MODIS albedo products have also been widely used for evaluating other satellite albedo products and land surface model outputs (Oleson et al., 2003; Wang et al., 2004). In this study, the MCD43C3 Collection 6 daily albedo product at spatial resolution of 0.05° is used.

GlobAlbedo: the GlobAlbedo project provides global surface albedo product at spatial resolutions of 1 km, 0.05° and 0.5° from 1998 to 2011. The product was generated with data from European satellites including SPOT4-VEGETATION, SPOT5-VEGETATION2 and Medium Resolution Imaging Spectrometer (MERIS) using an optimal estimation approach and a gap-filling scheme based on a ten-year climatology from MODIS BRDF (Muller et al., 2012; Potts et al., 2013). This product is on the 8-day interval with per pixel uncertainty information. The detailed description about the GlobAlbedo processing system can be found at <http://www.GlobAlbedo.org/>. The GlobAlbedo product at 0.05° spatial resolution is used in this study.

QA4ECV-albedo: the daily QA4ECV global albedo product was released recently by the Quality Assurance for Essential Climate variables (QA4ECV) project. The level 1 and level 2 data from several sensors including NOAA-AVHRR, several geostationary satellites and MODIS are used

as inputs to estimate two types of albedo bi-hemispherical diffuse reflectance and direct hemispherical reflectance over three broadbands (vis: 0.4-0.7 μ m; nir: 0.7- 3 μ m; sw: 0.4-3 μ m). There are three data products provided by the QA4ECV project: 1) AVHRR+GEO Broadband Albedo at 0.5° and 0.05°; 2) Spectral Albedo at 1km; and 3) Sea Ice Spectral Albedo at 1km. All these products are provided on a daily temporal resolution and cover the years from 1982 to 2016 with estimated uncertainties for every pixel. Detailed information on the algorithms and datasets can be found at <http://www.qa4ecv-land.eu/index.php>. The broadband daily albedo at 0.05° spatial resolution is used in the current study.

Regarding LAI datasets, MODIS, GLOBALMAP and QA4ECV LAI are used in this study and these three datasets are briefly introduced as follows.

MODIS-BNU-LAI: the LAI product from Beijing Normal University (Yuan et al., 2011) is used in the present study. Based on the original MOD15A2 LAI products (Justice et al., 2002; Myneni et al., 2002), this LAI product can provide temporally and spatially consistent MODIS LAI data compared to the original MODIS LAI that displays abrupt changes in the time series. It covers the time from 2000 to 2005 and provides LAI at 1 km every 8 days (Yuan et al., 2011).

GLOBMAP-LAI: the Global Mapping LAI product was generated through fusion of MODIS and AVHRR data quantitatively. The relationship between AVHRR and MODIS LAI for the overlapping period 2000-2006 was first established at pixel-level (Liu et al., 2012; Zhu et al., 2016). The relationship was then applied to construct AVHRR LAI back to 1981. The long-term LAI dataset was generated by fusing AVHRR and MODIS LAI datasets. The dataset was provided at 8km spatial resolution on a geographic grid.

QA4ECV-TIP-LAI: the LAI generated by QA4ECV project is based on QA4ECV albedo product and produced using the Two-stream Inversion Package (Clerici et al., 2010; Pinty et al., 2006; Voßbeck et al., 2010). The TIP retrieval, along with their uncertainties are retrieved in a highly efficient manner from look-up-tables (LUTs) of inversions of the Two-stream Model, which relates Bi- Hemispherical Reflectances (BHRs) to various canopy parameters and fluxes. The QA4ECV albedo dataset is used as the input to TIP, which provides long-term daily and monthly LAI as well as per-pixel uncertainty values at 0.5° and 0.05° from 1982 to 2016, of which the daily 0.05° product is used in this study. The QA4ECV-TIP-LAI is an effective LAI, computed by fitting a turbid medium model to the VIS and NIR Top-of-Canopy albedos (Two-Stream-model of Pinty et al. (2006)). Strictly, an inference on evaporating area based on effective LAI would have to take into account a canopy-dependent structure factor, which is neglected in this study. Also, the TIP model makes no clear separation between green and non-green canopy elements. Furthermore, the current QA4ECV-TIP-LAI version 1.0.1 is somewhat impaired through an apparent systematical inconsistency in the magnitude of the albedo product (see product users guide for reference, http://www.qa4ecv.eu/sites/default/files/D5.4_v1.0.pdf). In order to have maximum spatial and temporal coverage, none of the provided quality flags were applied for the present study and the uncertainty information was disregarded.

Table 1 lists detailed information of the LAI and land surface albedo datasets used in the current study. It should be noted that both LAI and albedo are linearly interpolated to model time step in the current study.

	Dataset	Temporal coverage	Temporal Resolution	Spatial Resolution
Albedo	MODIS	2000-now	Daily	0.05°
	GlobAlbedo	1998-2011	8 days	0.05°
	QA4ECV	1982-2016	daily	0.05°
LAI	MODIS	2000-now	8 days	0.01°
	GLOBMAP	1981-2017	8 days	0.08°
	QA4ECV	1982-2016	daily	0.05°

3.2 FLUXNET measurements

Standard meteorological measurements and surface fluxes measured with eddy covariance instruments from the FLUXNET network (Baldocchi, 2003) are used to drive HOLAPS model and validate the simulation results. Table 2 lists the FLUXNET sites used in the current study. They are a subset of all FLUXNET sites, which are selected by the criteria: 1) the site has less than 20% missing data, 2) all the inputs required by HOLAPS models are available. All the FLUXNET measurements are quality checked and the quality flags are applied to obtain the highest quality of measurements. These sites are located in different areas around the world and can represent a wide range of climate and surface conditions. The reference listed in Table 2 describes the detailed information for each site. The lack of closure in the energy balance for eddy-covariance measurements are solved in the current study with a simple energy balance correction method proposed by Twine et al. (2000).

Table 2. List of the FLUXNET sites used in this study with their FLUXNET code (ID), and reference. The symbol ‘+’ in the years column denotes the years having observations for each site.

ID	Latitude	Longitude	2003	Years 2004	2005	Reference
AT-Neu	47.12N	11.32E	+	+		(Wohlfahrt et al., 2008)
AU-How	12.49S	131.15E	+	+	+	(Hutley et al., 2000)
AU-Tum	35.66S	148.15E	+	+	+	(Leuning et al., 2005)
BE-Bra	51.31N	4.52E		+	+	(Gond et al., 1999)
BE-Vie	50.31N	6.00E			+	(Aubinet et al., 2001)
CA-Man	55.88N	98.48W	+			(Dunn et al., 2007)
CA-Mer	45.41N	75.52W	+	+		(Lafleur, 2003)
CA-NS1	55.88N	98.48W	+	+		(Gouldon et al., 2006)
CA-NS2	55.91N	98.52W	+	+	+	(Gouldon et al., 2006)
CA-NS3	55.91N	98.38W		+	+	(Gouldon et al., 2006)
CA-NS4	55.91N	98.38W	+			(Gouldon et al., 2006)
CA-NS5	55.86N	98.49W	+	+	+	(Gouldon et al., 2006)
CA-NS6	55.92N	98.96W	+	+	+	(Gouldon et al., 2006)
CA-NS7	56.64N	99.95W	+	+		(Gouldon et al., 2006)
CA-Qcu	49.27N	74.04W	+	+	+	
CA-SF3	54.09N	106.01W	+	+	+	(Mkhabela et al., 2009)
CH-Oel	47.29N	7.73E	+			(Gilmanov et al., 2007)
CZ-BK1	49.50N	18.54E			+	
DE-Gri	50.95N	13.51E			+	(Gilmanov et al., 2007)
DE-Hai	51.08N	10.45E	+	+	+	(Knohl et al., 2003)
DE-Meh	51.28N	10.66E		+	+	(Scherer-Lorenzen et al., 2007)
DE-Tha	50.96N	13.57E	+	+	+	
DE-Wet	50.45N	11.46E	+	+	+	(Rebmann et al., 2010)
FR-Hes	48.67N	7.06E	+	+	+	(Granier et al., 2000)
FR-LBr	44.72N	0.77W	+			(Berbigier et al., 2001)
FR-Pue	43.74N	3.60E		+	+	(Allard et al., 2008)
HU-Bug	46.69N	19.60E	+	+	+	(Nagy et al., 2007)
IT-Cpz	41.71N	12.38E		+	+	(Garbalsky et al., 2008)
IT-Ro2	42.39N	11.92E		+		(Tedeschi et al., 2006)
IT-SRo	43.73N	10.28E	+			(Chiesi et al., 2005)
NL-Cal	51.97N	4.93E	+	+	+	(Beljaars and Bosveld, 1997)
NL-Loo	52.17N	5.74E	+		+	(Dolman et al., 2002)
US-ARM	36.61N	97.49W	+	+	+	(Fischer et al., 2007)
US-Aud	31.59N	110.51W		+	+	(Tang et al., 2011a; Yang et al., 2008)
US-Bkg	44.35N	96.84W		+	+	(Zhang et al., 2008)
US-Bo1	40.01N	88.29W	+	+	+	(Meyers, 2004)
US-FPe	48.31N	105.10W	+		+	(Gilmanov et al., 2005; Zhang et al., 2008)
US-Goo	34.25N	89.87W		+		
US-Ho1	45.20N	68.74W	+	+		(Hollinger et al., 2004)

US-Ho2	45.21N	68.75W	+	+		(Hollinger et al., 2004)
US-Los	46.08N	89.98W	+	+	+	
US-MOz	38.74N	92.20W			+	(Gu et al., 2007; Gu et al., 2006)
US-Ne1	41.17N	96.48W	+	+		(Verma et al., 2005)
US-Ne2	41.16N	96.47W	+	+		(Verma et al., 2005)
US-Ne3	41.18N	96.44 W	+	+		(Verma et al., 2005)
US-Oho	41.55N	83.84 W		+	+	
US-Ton	38.43N	120.97W	+		+	(Baldocchi et al., 2004)
US-WCr	45.81N	90.08W	+		+	(Cook et al., 2004)

4 Results and discussion

4.1 Sensitivity of HOLAPS to albedo and LAI

The sensitivity of HOLAPS simulated LE and H to albedo and LAI are shown in Figures 1 and 2, where the plots display the variation of the relative error between unperturbed and perturbed albedo and LAI for each uncertainty level. In general, the large range of relative error denotes that HOLAPS is more sensitive to that variable. The relative errors for both LE and H increase linearly with the increase of uncertainty in both albedo and LAI. The relative error of LE is more sensitive to uncertainty in LAI than that in albedo. The relative error of LE caused by changes of albedo is less than 10% while the relative error can reach 20% for LAI. Regarding H, the change of relative errors is similar due to the change of LAI and albedo, with largest relative error around 20%. It is noted that a more rigorous sensitivity/uncertainty analysis as suggested by Pianosi et al. (2016) is needed to disentangle the issues of forcing uncertainty on flux estimation,

which needs synthetic data and comprehensive sensitivity analysis (Saltelli, 1999; Saltelli et al., 2010).

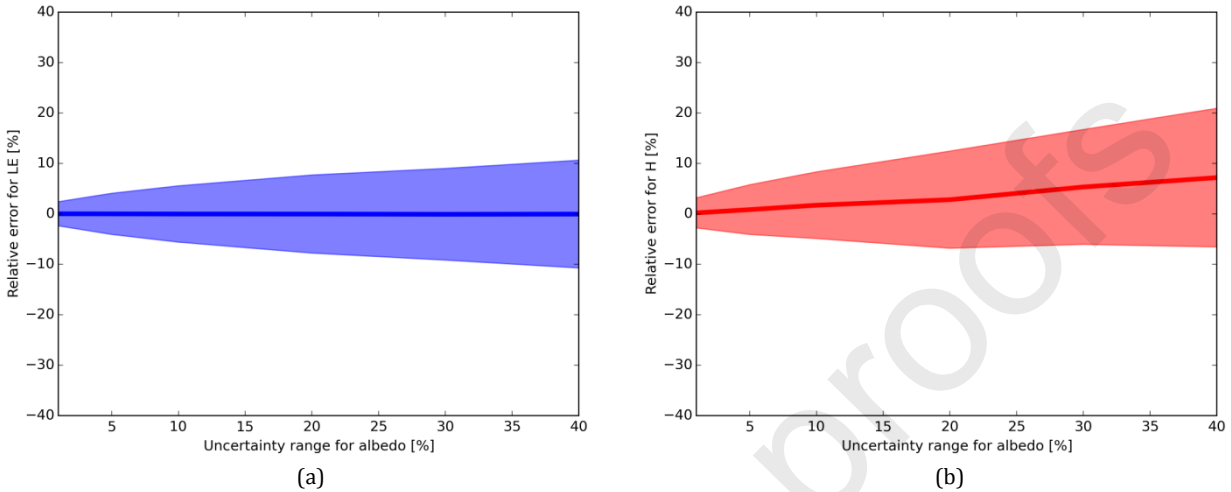


Figure 1: Sensitivity of HOLAPS to albedo with a range of added uncertainty. The shaded area represents standardized deviation of the mean relative error which is shown with bold line. (a) relative error of simulated LE; (b) relative error of simulated H.

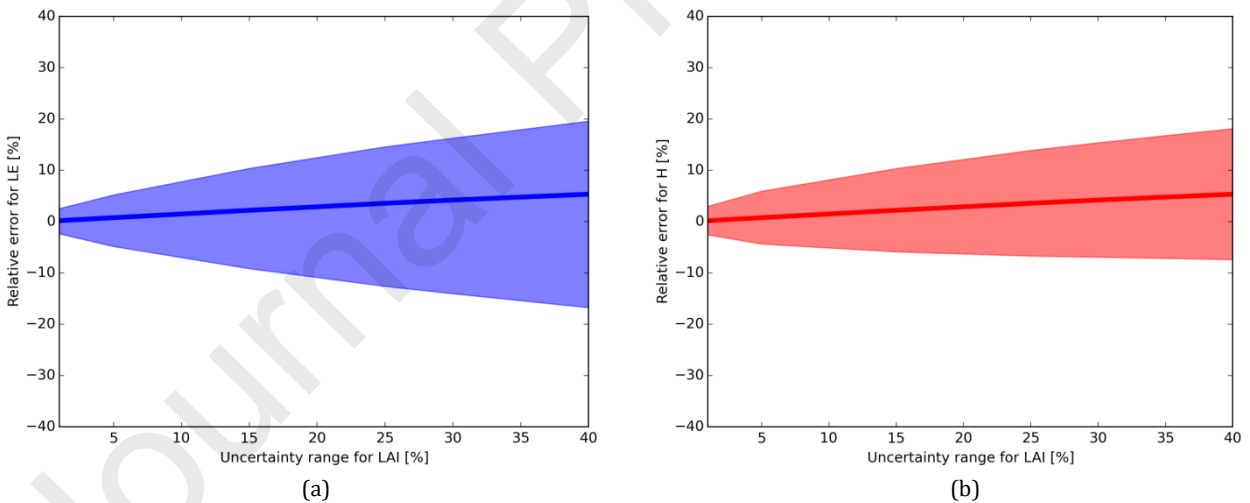


Figure 2: Sensitivity of HOLAPS to LAI with a range of added uncertainty. The shaded area represents standardized deviation of the mean relative error which is shown with bold line. (a) relative error of simulated LE; (b) relative error of simulated H.

4.2 Evaluation of latent/sensible heat fluxes based on MODIS albedo and LAI datasets

The estimated latent and sensible heat fluxes from HOLAPS with MODIS albedos and LAIs are evaluated with FLUXNET measurements. The validation results are shown in Figure 3, where

the related statistics are also summarized. Overall, the HOLAPS latent heat flux estimates agree well with FLUXNET measurements with RMSD of 51.1, 30.7 and 26.3 W/m², cRMSD of 48.9, 26.8, and 21.7 W/m², Bias of 14.6, 14.8, and 14.9 W/m², R² of 0.75, 0.72 and 0.67 for flux estimates at hourly, daily and monthly scale respectively. It can be seen that the accuracy level largely increases with the time scales, which indicates that the uncertainties associated with heat flux estimation can be minimized at longer timescales. All correlations are statistically significant with p value less than 0.05. The error scores are also comparable with the accuracy level reported by previous studies such as Ershadi et al. (2014), Michel et al. (2016) and McCabe et al. (2016). In terms of error scores of sensible heat flux, to the best of our knowledge, the global sensible heat flux has rarely been validated against FLUXNET measurements. Previous studies normally estimate sensible heat flux at regional scale and validate against limited in-situ measurements. The accuracy of sensible heat flux found by these studies has a wide range from ~10 W/m² to ~100 W/m² (Jia et al., 2003; Marx et al., 2008; Tang et al., 2011b; Wang et al., 2013; Zhuang et al., 2016). In this study, the sensible heat flux from HOLAPS was validated in the same way as the latent heat flux. The R², RMSD and cRMSD values are also shown in Figure 3, which are worse than the ones for latent heat flux at hourly and daily time scale. The RMSD, cRMSD and R² range from 79.2 (hourly) to 35.6 (daily) W/m², 78.0 (hourly) to 32.9 (daily) W/m², 0.54 (hourly) to 0.47 (daily). However, the error statistics for monthly fluxes are comparable between sensible and latent flux estimates, with RMSD of 25.7 W/m², cRMSD of 21.4 W/m² and R² of 0.65. Compared to the models that use prescribed albedo values and satellite-based methods that suffer from clouds, HOLAPS framework has the advantages of providing continuous high temporal/spatial resolution estimates of water and energy fluxes with comparable accuracy as existing satellite-based estimates. In order to generate long-term heat

fluxes within the HOLAPS framework, MODIS albedo and LAI products need to be replaced by long-term albedo and LAI datasets. The following section investigates the accuracy achieved by HOLAPS with different albedo and LAI datasets. The above evaluation scores based on MODIS data are considered as the baseline accuracy to be compared with the estimates based on other long-term albedo and LAI datasets.

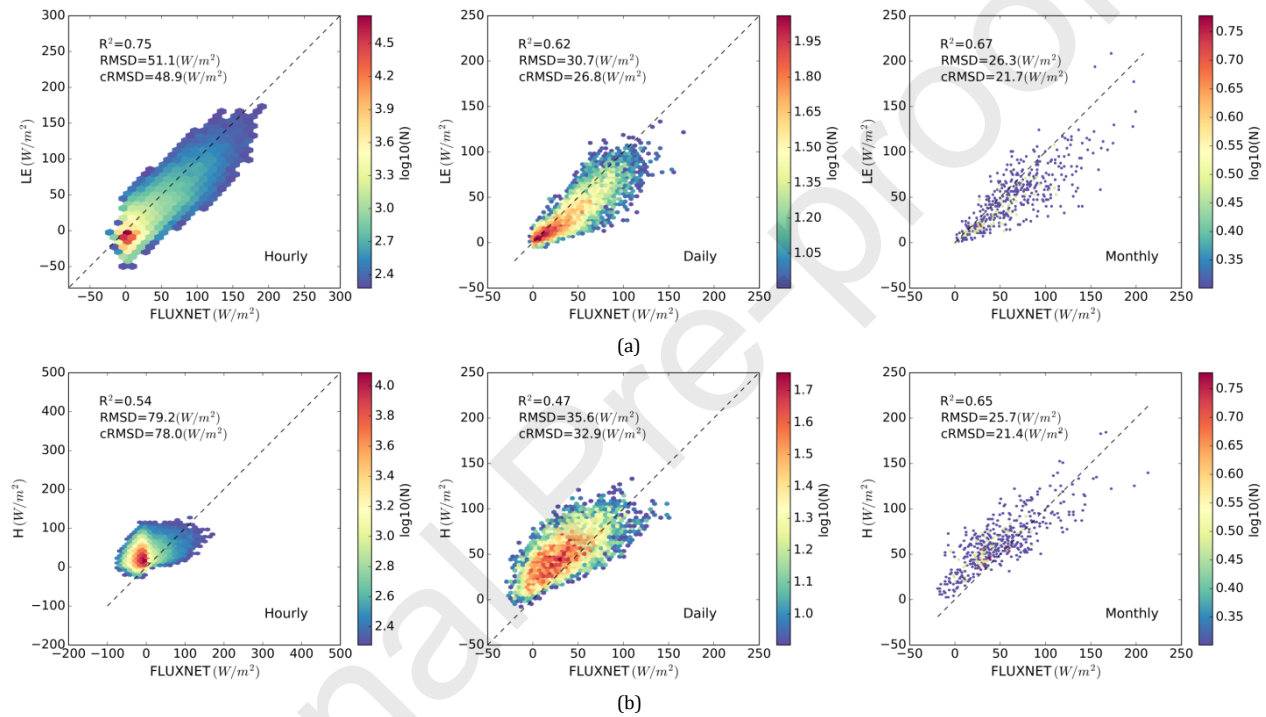


Figure 3: Comparison between FLUXNET measurements and HOLAPS latent heat flux (a) and sensible heat flux (b) estimates based on MODIS albedo and LAI. The colors denote the occurrence frequency of values with unit of W/m^2 .

4.3 Evaluation of latent/sensible heat fluxes based on different albedo and LAI datasets

The GlobAlbedo, QA4ECV, and GLOBMAP are used to replace MODIS albedo/LAI datasets for estimating latent and sensible heat fluxes. Tables 3 and 4 respectively summarize the statistical scores for latent and sensible heat fluxes based on entire FLUXNET data record. Compared to the error scores of estimates from MODIS albedo (Figure 3), the GlobAlbedo and

QA4ECV albedo show quite similar performance for both latent and sensible heat fluxes. For LAI, the GLOBMAP also shows comparable results compared to MODIS for both latent and sensible heat fluxes. However, the QA4ECV LAI leads to much worse performance for latent heat flux and slightly worse performance for sensible heat flux. It is likely due to the fact that QA4ECV LAI is effective LAI rather than green leaf LAI, which are represented by MODIS and GLOBMAP LAI. The results also suggest the possibility of using QA4ECV albedo and GLOBMAP LAI for estimating long-term latent/sensible heat fluxes with HOLAPS. Model performance statistics are summarized in the bottom row of Table 3 and 4, which show the comparable error scores compared to MODIS.

Table 3: Summary of comparisons between FLUXNET LE measurements and HOLAPS LE estimation based on different albedo and LAI datasets at hourly (h), daily (d) and monthly (m) timescales. The numbers in bold font refer to the best performance within that column.

Variables		RMSD (W/m ²)			cRMSD (W/m ²)			R ²		
		h	d	m	h	d	m	h	d	m
Albedo	GlobAlbedo	51.2	30.7	26.3	49.1	26.9	21.8	0.76	0.62	0.66
	QA4ECV	51.0	31.2	27.0	48.3	26.6	21.5	0.76	0.62	0.67
LAI	GLOBMAP	54.1	33.4	29.3	51.4	28.7	23.9	0.72	0.58	0.61
	QA4ECV	64.4	42.9	39.1	57.4	31.3	25.3	0.64	0.40	0.48
Albedo/LAI	MODIS	51.1	30.7	26.3	48.9	26.8	21.7	0.75	0.62	0.67
	QA4ECV/ GLOBMAP	54.0	33.9	30.0	50.7	28.3	23.5	0.74	0.58	0.61

Table 4: Summary of comparisons between FLUXNET H measurements and HOLAPS H estimation based on different albedo and LAI datasets at hourly (h), daily (d) and monthly (m) timescales. The numbers in bold font refer to the best performance within that column.

Variables		RMSD (W/m ²)			cRMSD (W/m ²)			R ²		
		h	d	m	h	d	m	h	d	m
Albedo	GlobAlbedo	79.1	36.0	26.2	77.9	33.0	21.6	0.53	0.46	0.64
	QA4ECV	81.5	34.9	24.2	80.9	33.4	21.9	0.50	0.45	0.64
LAI	GLOBMAP	78.9	36.4	26.9	77.4	32.8	21.4	0.48	0.62	0.66
	QA4ECV	80.9	40.1	30.5	78.1	34.1	21.7	0.50	0.38	0.52
Albedo/LAI	MODIS	79.2	35.6	25.7	78.0	32.9	21.4	0.54	0.47	0.65
	QA4ECV/ GLOBMAP	80.5	33.9	24.5	79.6	28.3	21.5	0.52	0.58	0.66

In addition to the validation based on the entire data record from all FLUXNET stations, the comparison is also conducted for each station. The error scores including RMSD, cRMSD and R for each station are shown in Figure 4 for latent heat flux and Figure 5 for sensible heat flux in the form of box plots. The corresponding mean and standard deviation values are summarized in Tables 5 and 6. It can be seen that similar results are obtained as the statistics based on the entire data record. All three albedo datasets give similar error scores, while GLOBMAP and MODIS-BNU-LAI also show comparable results. The QA4ECV LAI leads to worse error scores due to its use of effective LAI and possibly other factors described in section 3. The combined use of QA4ECV albedo and GLOBMAP LAI shows similar performance for latent/sensible heat fluxes to that based on MODIS albedo and LAI. It further suggests the possibility of generating long-term latent/sensible heat fluxes from the combined use of QA4ECV albedo and GLOBMAP LAI.

Overall, we can conclude that the latent/sensible heat fluxes estimated from HOLAPS are not very sensitive to different albedo inputs that have different temporal and spatial resolutions. However, the LAI has more impact on the estimation of latent heat flux, which are in accordance with the study by Richard et al. (2018), who found that the large differences in LAI can lead to substantial uncertainties in carbon and water fluxes simulation. The current study also helps to select QA4ECV albedo and GLOBMAP LAI as the forcing to derive latent/heat flux with HOLAPS. QA4ECV provides newly developed long-term high resolution albedo product and can be recognized as the updated version of GlobAlbedo dataset (Nightingale et al., 2018), while GLOBMAP provides updated LAI dataset based on MODIS and AVHRR products (Liu et al., 2012; Zhu et al., 2016). Nevertheless, it should be noted that surface albedo has strong diurnal variation compared to LAI which is varying slowly in time (Wang et al., 2016). The existing

satellite-based albedo datasets are normally at daily or multiday temporal resolution, which might induce errors in retrieved energy fluxes at sub-daily scale, although they have been used for estimating evapotranspiration via model simulation or satellite retrieval. The temporal interpolation scheme applied to daily satellite-based albedo dataset in HOLAPS framework might incur discrepancies between estimated and measured energy fluxes at sub-daily scales. In order to improve the accuracy of simulated latent/sensible heat fluxes, diurnal cycle albedo dataset is highly required. Several recent studies such as (Wang et al., 2015; Wang et al., 2016) have investigated the issue of albedo diurnal changes and developed new daily albedo products that take into account its diurnal patterns. The generation of operational sub-daily surface albedo dataset will support the model and remote sensing community to better estimate water and energy fluxes.

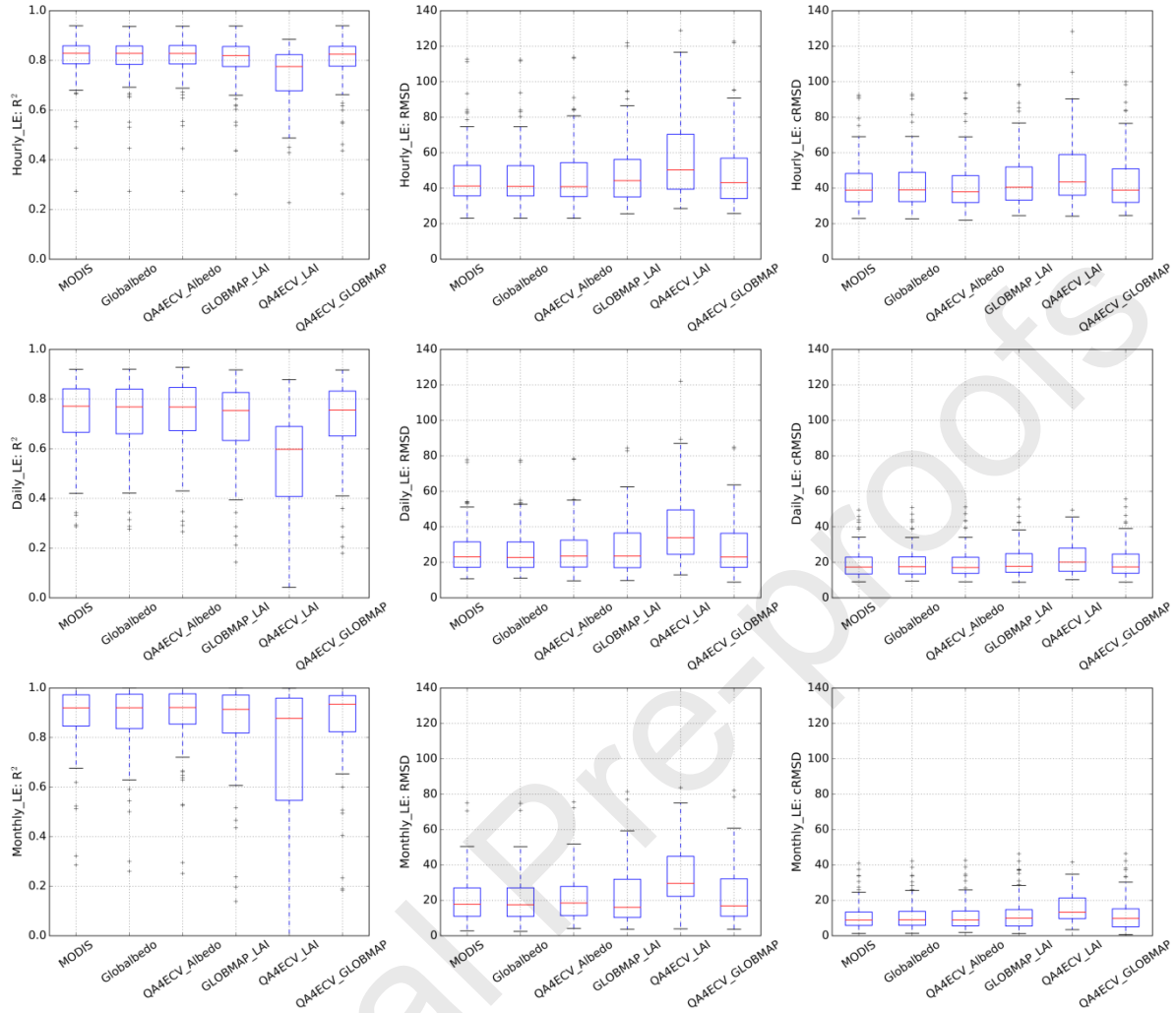


Figure 4: Box plots for validation statistics that are calculated at each FLUXNET station for latent heat flux (LE) at hourly, daily and monthly timescales. The red line indicates the median value, and the unit for RMSD and cRMSD are W/m^2 .

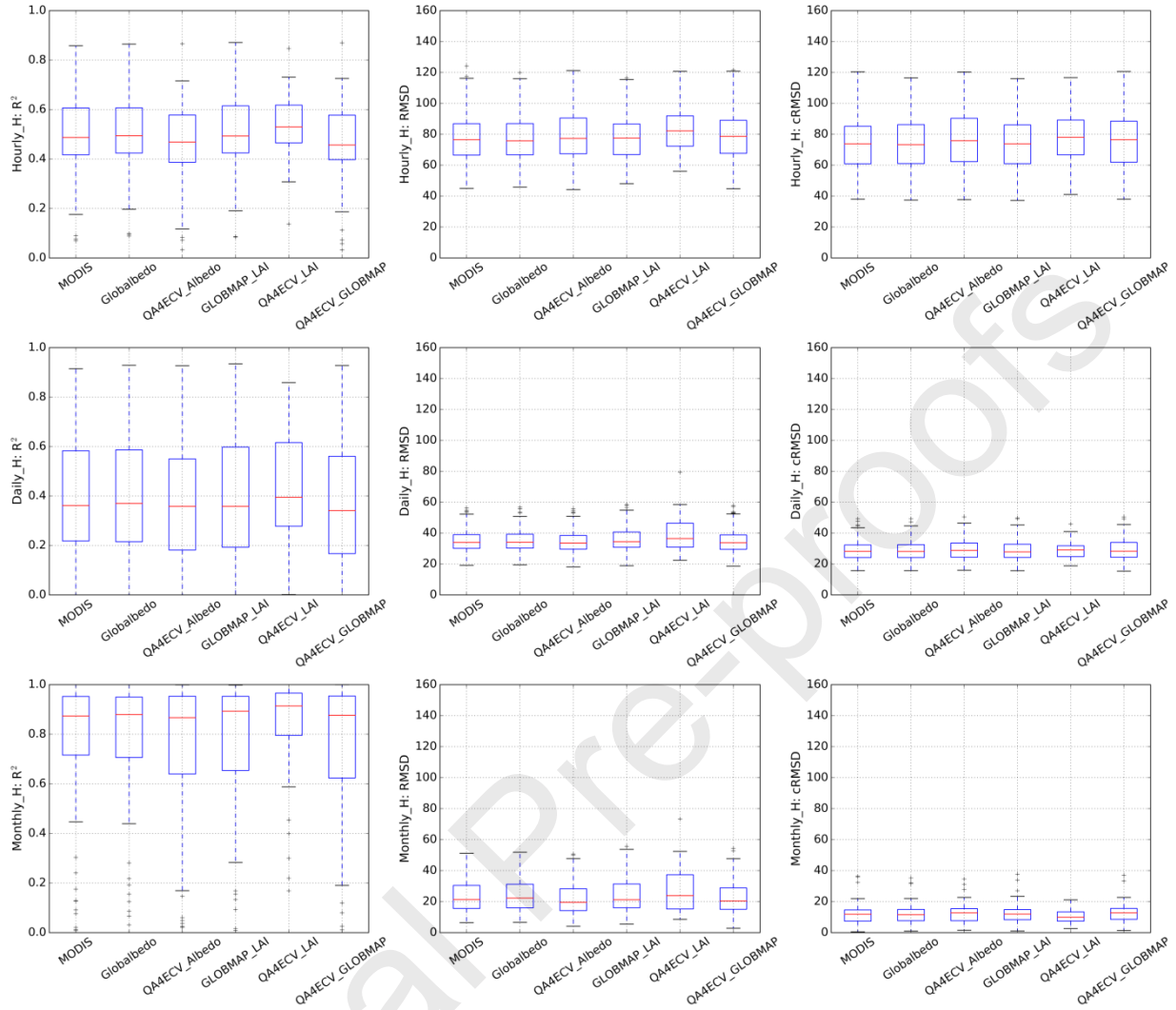


Figure 5: Box plots for sensible heat flux (H) at hourly, daily and monthly timescales.

Table 5. Summary of the mean and standardized deviation of box plots in Figure 4.

Variables	RMSD (W/m ²)			cRMSD (W/m ²)			R ²		
	h	d	m	h	d	m	h	d	m
MODIS	46.4 ± 17.2	26.5 ± 13.2	21.2 ± 13.9	42.6 ± 14.5	19.4 ± 8.1	11.2 ± 8.0	0.81 ± 0.10	0.74 ± 0.14	0.88 ± 0.13
GlobAlbedo	46.6 ± 17.2	26.5 ± 13.2	21.2 ± 13.9	42.8 ± 14.6	19.5 ± 8.2	11.3 ± 8.1	0.80 ± 0.09	0.74 ± 0.14	0.88 ± 0.14
QA4ECV_Albedo	46.3 ± 17.5	27.1 ± 13.3	22.1 ± 13.9	42.1 ± 14.8	19.4 ± 8.2	11.3 ± 8.1	0.81 ± 0.10	0.74 ± 0.14	0.88 ± 0.14
GLOBMAP_LAI	48.6 ± 18.8	28.0 ± 14.8	22.5 ± 16.1	44.6 ± 15.6	20.7 ± 8.9	12.4 ± 9.4	0.79 ± 0.11	0.71 ± 0.16	0.86 ± 0.17
QA4ECV_LAI	59.4 ± 27.2	38.6 ± 20.6	33.5 ± 17.3	50.4 ± 20.9	22.5 ± 9.3	15.3 ± 8.4	0.74 ± 0.12	0.55 ± 0.19	0.72 ± 0.32
QA4ECV/ GLOBMAP	48.2 ± 19.2	28.4 ± 15.0	23.2 ± 16.1	43.8 ± 15.8	20.5 ± 9.0	12.3 ± 9.4	0.79 ± 0.11	0.71 ± 0.16	0.86 ± 0.17

Table 6. Summary of the mean and standardized deviation of box plots in Figure 5.

Variables	RMSD (W/m ²)			cRMSD (W/m ²)			R ²		
	h	d	m	h	d	m	h	d	m
MODIS	77.4 ± 16.3	35.3 ± 7.6	23.5 ± 10.2	74.0 ± 18.3	28.6 ± 6.7	12.0 ± 6.3	0.50 ± 0.15	0.40 ± 0.23	0.74 ± 0.32
GlobAlbedo	77.3 ± 16.0	35.6 ± 7.7	24.0 ± 10.4	73.8 ± 18.2	28.5 ± 6.6	12.0 ± 6.2	0.50 ± 0.14	0.40 ± 0.23	0.74 ± 0.32
QA4ECV_Albedo	78.9 ± 17.5	34.6 ± 7.9	22.0 ± 10.2	76.2 ± 19.2	29.0 ± 6.8	12.6 ± 6.0	0.47 ± 0.15	0.37 ± 0.23	0.73 ± 0.32
GLOBMAP_LAI	77.6 ± 15.4	35.9 ± 8.0	24.3 ± 11.0	73.9 ± 17.8	28.6 ± 6.6	12.3 ± 6.0	0.50 ± 0.15	0.40 ± 0.24	0.73 ± 0.32
QA4ECV_LAI	82.4 ± 14.2	38.5 ± 10.0	26.6 ± 14.3	77.4 ± 17.2	29.0 ± 5.5	10.9 ± 5.2	0.53 ± 0.12	0.43 ± 0.21	0.83 ± 0.23
QA4ECV/ GLOBMAP	79.0 ± 17.1	34.8 ± 8.0	22.2 ± 10.5	76.2 ± 18.9	29.1 ± 6.8	12.7 ± 5.9	0.46 ± 0.16	0.37 ± 0.24	0.72 ± 0.33

4.4 Performance of latent/sensible heat fluxes over different land covers

In addition, we investigate the impact of land cover on the accuracy of estimated latent/sensible heat fluxes. Figures 6 and 7 show the HOLAPS error scores for each land cover type for latent and sensible heat fluxes respectively. In general, the latent heat flux shows stable performance over different land covers, with relatively high RMSD values (larger than 65 W/m²) over deciduous broadleaf forests and savannas. Compared to latent heat flux, the sensible heat flux shows worse error scores for all land cover types that can also be seen from statistics based on the entire data record. Nevertheless, the sensible heat flux also displays similar performance over different land covers except evergreen needleleaf forest with RMSD of 96.1 W/m². Taken together, these results suggest that there are no systematic differences between model performance with different land covers. However, there are still uncertainties associated with HOLAPS estimates, which are caused by model uncertainties, reference data uncertainties, forcing uncertainties and scale mismatches. These challenges remain to be addressed in future studies.

433

434

Journal Pre-proofs

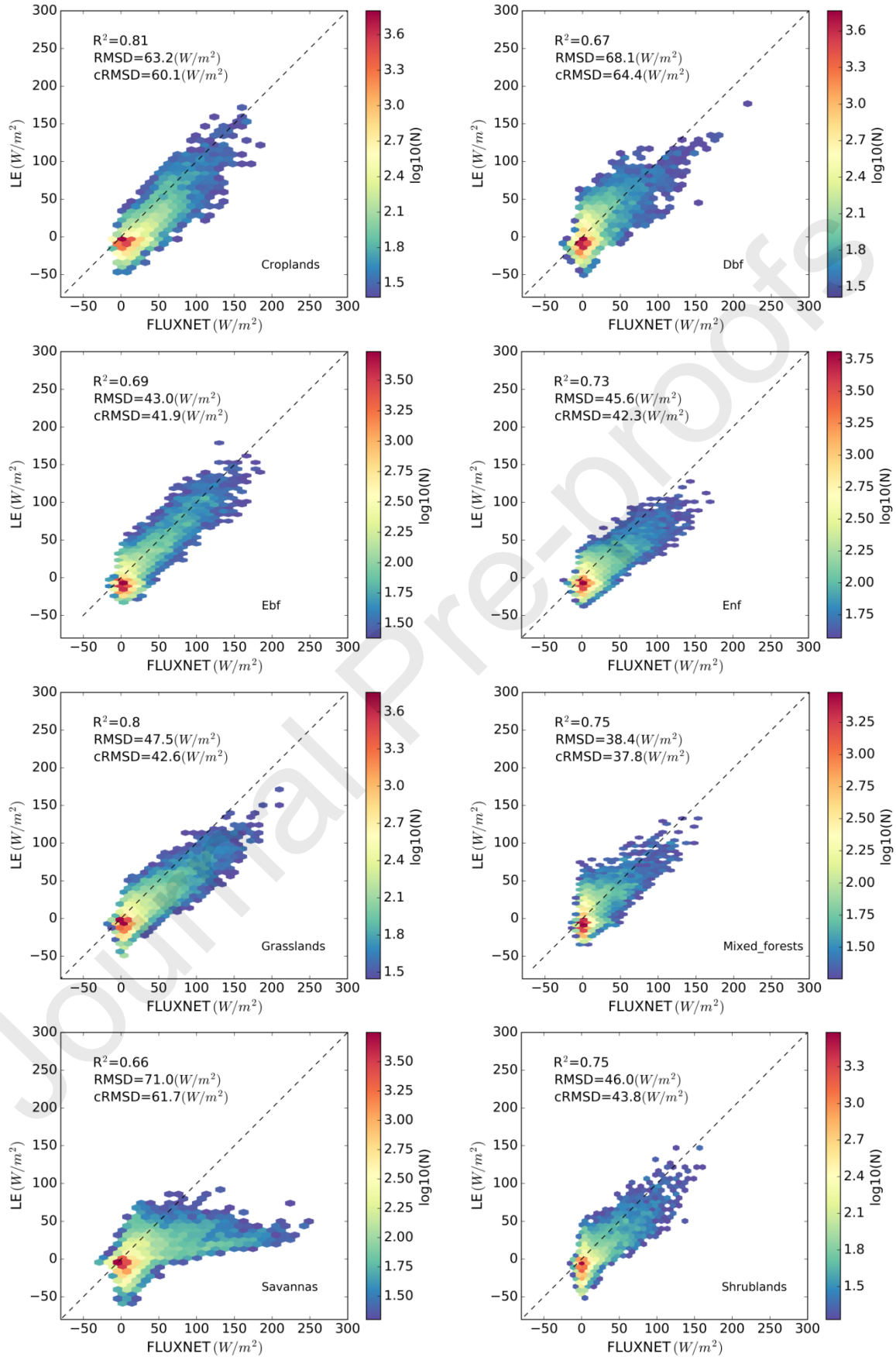


Figure 6: The performance of latent heat flux estimated based on QA4ECV albedo and GLOBMAP LAI for different land covers. Dbf is short for deciduous broadleaf forest, Ebf is evergreen broadleaf forest and Enf is evergreen needleleaf forest.

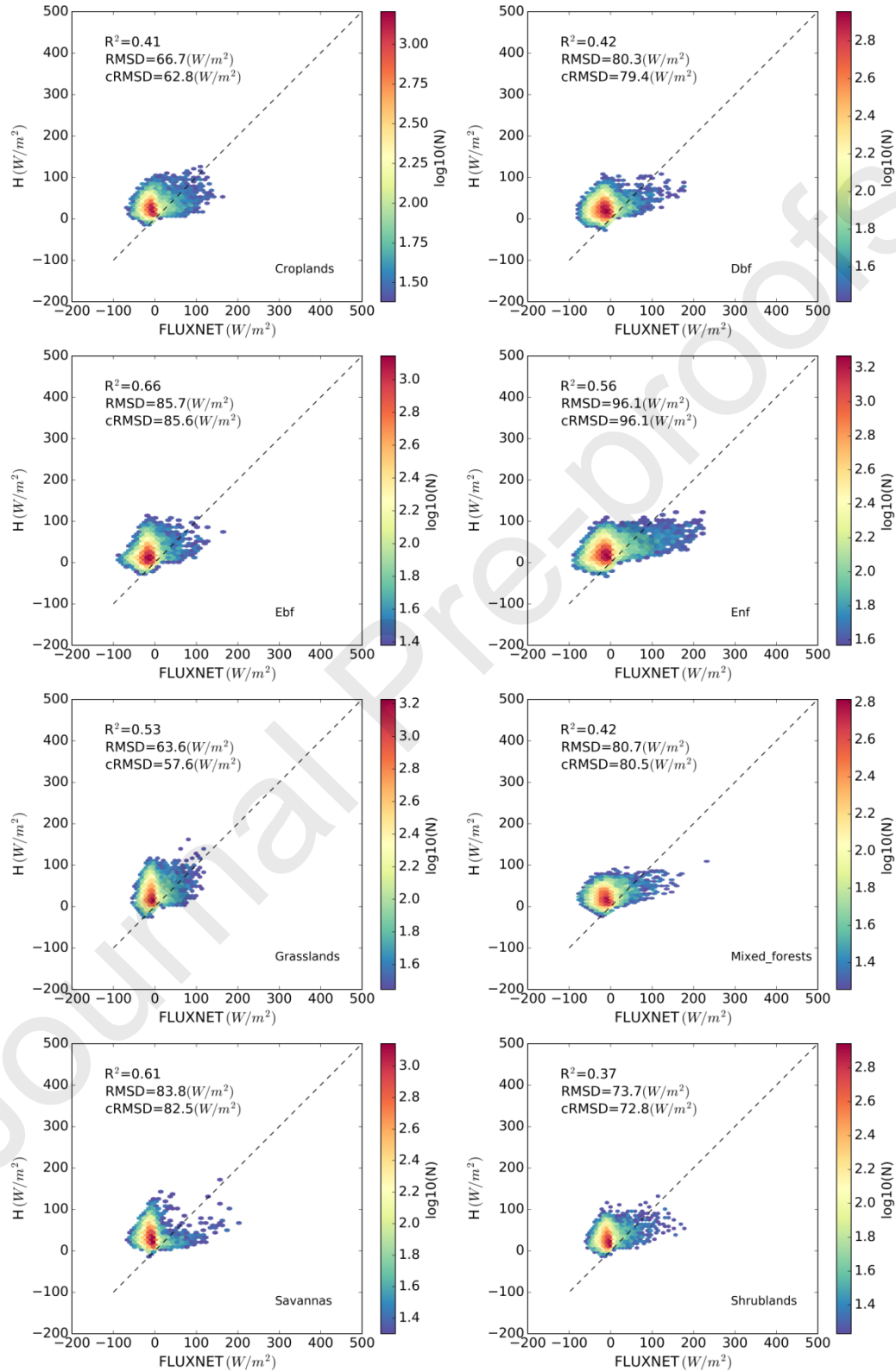


Figure 7: The performance of sensible heat flux estimated based on QA4ECV albedo and GLOBMAP LAI for different land covers. Dbf is short for deciduous broadleaf forest, Ebf is evergreen broadleaf forest and Enf is evergreen needleleaf forest.

5 Conclusions

In this study, the sensitivity of latent/sensible heat fluxes estimated from the HOLAPS model to different long-term global albedo and LAI datasets are explored. The latent/sensible heat fluxes driven by MODIS albedo and LAI are taken as reference. For latent heat flux, the RMSD is 51.1 (26.3) W/m^2 with R^2 of 0.75 (0.67) for hourly (monthly) time scales, while the RMSD is 79.2 (25.7) W/m^2 with R^2 of 0.54 (0.65) for sensible heat flux. Compared to this reference, the accuracy of the HOLAPS model is found to be comparable to results reported by other studies. MODIS albedo and LAI were then replaced by QA4ECV, GlobAlbedo and GLOBMAP to investigate their impacts on the estimated latent and sensible heat fluxes by HOLAPS. The results showed that all albedo datasets lead to comparable latent/sensible heat fluxes estimates, while the choice of the LAI dataset has a greater impacts on estimated heat fluxes. Among different LAI datasets considered in this study, QA4ECV-TIP-LAI shows the worst performance due to its characteristic as (optically) effective LAI and other factors, as anticipated in the dataset description in section 3. Finally, the combination of QA4ECV albedo and GLOBMAP LAI was used for estimating latent and sensible heat fluxes, and the error scores (e.g., $\text{RMSD} = 54 \text{ W/m}^2$, $R^2 = 0.74$ for hourly latent heat flux, $\text{RMSD} = 80.5 \text{ W/m}^2$, $R^2 = 0.52$ for hourly sensible heat flux) were found to be comparable to MODIS estimates. Therefore, taking the advantages of being long-term and the high spatial resolution of QA4ECV albedo and GLOBMAP LAI, as well as the comparable accuracy of heat fluxes estimation to MODIS, our findings suggest that the

QA4ECV albedo and GLOBMAP LAI datasets have the potential to be used to generate long-term high resolution global latent and sensible heat fluxes with HOLAPS framework.

Acknowledgments

The present study was supported by QA4ECV (EU FP7 Project Quality Assurance for Essential Climate Variables (QA4ECV), grant no. 607405, <http://www.qa4ecv-land.eu/index.php>). We thank the PIs for all FLUXNET stations and the dissemination of FLUXNET data (<https://fluxnet.fluxdata.org>). We also thank Beijing Normal University for the provision of the enhance MODIS LAI data (<http://globalchange.bnu.edu.cn/research/lai>), and the MODIS land team (<https://modis.gsfc.nasa.gov/data/dataproduct/>), the ESA GlobAlbedo project team (<http://www.globalbedo.org>), GLOBMAP team (http://www.globalmapping.org/globalLAI/GLOBMAPLAI_Version3/) for their efforts on the distribution of corresponding albedo and LAI datasets.

References

- Allard, V., Ourcival, J.M., Rambal, S., Joffre, R., Rocheteau, A., 2008. Seasonal and annual variation of carbon exchange in an evergreen Mediterranean forest in southern France. *Global Change Biology*, 14(4): 714-725.
- Allen, R.G., Pereira, L.S., Raes, D., Smith, M., 1998. Crop evapotranspiration-Guidelines for computing crop water requirements-FAO Irrigation and drainage paper 56. FAO, Rome, 300(9): D05109.
- Aubinet, M. et al., 2001. Long term carbon dioxide exchange above a mixed forest in the Belgian Ardennes. *Agricultural and Forest Meteorology*, 108(4): 293-315.
- Badgley, G., Fisher, J.B., Jiménez, C., Tu, K.P., Vinukollu, R., 2015. On uncertainty in global terrestrial evapotranspiration estimates from choice of input forcing datasets. *Journal of Hydrometeorology*, 16(4): 1449-1455.
- Baldocchi, D., 2008. 'Breathing' of the terrestrial biosphere: lessons learned from a global network of carbon dioxide flux measurement systems. *Australian Journal of Botany*, 56(1): 1-26. DOI:<http://dx.doi.org/10.1071/BT07151>
- Baldocchi, D. et al., 2001. FLUXNET: A New Tool to Study the Temporal and Spatial Variability of Ecosystem-Scale Carbon Dioxide, Water Vapor, and Energy Flux Densities. *Bulletin of the American Meteorological Society*, 82(11): 2415-2434.
- Baldocchi, D.D., 2003. Assessing the eddy covariance technique for evaluating carbon dioxide exchange rates of ecosystems: past, present and future. *Global Change Biology*, 9(4): 479-492.
- Baldocchi, D.D., Xu, L., Kiang, N., 2004. How plant functional-type, weather, seasonal drought, and soil physical properties alter water and energy fluxes of an oak-grass savanna and an annual grassland. *Agricultural and Forest Meteorology*, 123(1-2): 13-39.

- Beljaars, A., Bosveld, F., 1997. Cabauw data for the validation of land surface parameterization schemes. *Journal of Climate*: 1172-1193.
- Berbigier, P., Bonnefond, J.-m., Mellmann, P., 2001. CO₂ and water vapour fluxes for 2 years above Euroflux forest site. *Agricultural and Forest Meteorology*, 108(3): 183-197.
- Betts, A.K., Ball, J.H., Beljaars, A., Miller, M.J., Viterbo, P.A., 1996. The land surface-atmosphere interaction: A review based on observational and global modeling perspectives. *Journal of Geophysical Research: Atmospheres*, 101(D3): 7209-7225.
- Cescatti, A. et al., 2012. Intercomparison of MODIS albedo retrievals and in situ measurements across the global FLUXNET network. *Remote sensing of environment*, 121: 323-334.
- Chiesi, M. et al., 2005. Modelling carbon budget of Mediterranean forests using ground and remote sensing measurements. *Agricultural and Forest Meteorology*, 135(1-4): 22-34.
- Clerici, M. et al., 2010. Consolidating the Two-Stream Inversion Package (JRC-TIP) to Retrieve Land Surface Parameters From Albedo Products. *IEEE Journal of Selected Topics in Applied Earth Observations and Remote Sensing*, 3(3): 286-295. DOI:10.1109/JSTARS.2010.2046626
- Cook, B.D. et al., 2004. Carbon exchange and venting anomalies in an upland deciduous forest in northern Wisconsin, USA. *Agricultural and Forest Meteorology*, 126(3-4): 271-295.
- Courault, D., Seguin, B., Olioso, A., 2005. Review on estimation of evapotranspiration from remote sensing data: From empirical to numerical modeling approaches. *Irrigation and Drainage systems*, 19(3-4): 223-249.
- Dolman, A.J., Moors, E.J., Elbers, J.A., 2002. The carbon uptake of a mid latitude pine forest growing on sandy soil. *Agricultural and Forest Meteorology*, 111(3): 157-170.
- Dunn, A.L., Barford, C.C., Wofsy, S.C., Goulden, M.L., Daube, B.C., 2007. A long-term record of carbon exchange in a boreal black spruce forest: means, responses to interannual variability, and decadal trends. *Global Change Biology*, 13(3): 577-590.
- Ershadi, A., McCabe, M., Evans, J.P., Chaney, N.W., Wood, E.F., 2014. Multi-site evaluation of terrestrial evaporation models using FLUXNET data. *Agricultural and Forest Meteorology*, 187: 46-61.
- Fischer, M.L., Billesbach, D.P., Berry, J.a., Riley, W.J., Torn, M.S., 2007. Spatiotemporal Variations in Growing Season Exchanges of CO₂, H₂O, and Sensible Heat in Agricultural Fields of the Southern Great Plains. *Earth Interactions*, 11(17): 1-21.
- Fisher, J.B. et al., 2017. The future of evapotranspiration: Global requirements for ecosystem functioning, carbon and climate feedbacks, agricultural management, and water resources. *Water Resources Research*, 53(4): 2618-2626.
- Fisher, J.B., Tu, K.P., Baldocchi, D.D., 2008. Global estimates of the land-atmosphere water flux based on monthly AVHRR and ISLSCP-II data, validated at 16 FLUXNET sites. *Remote Sensing of Environment*, 112(3): 901-919. DOI:<http://dx.doi.org/10.1016/j.rse.2007.06.025>
- Garbulsky, M.F., Peñuelas, J., Papale, D., Filella, I., 2008. Remote estimation of carbon dioxide uptake by a Mediterranean forest. *Global Change Biology*, 14(12): 2860-2867. DOI:10.1111/j.1365-2486.2008.01684.x

- Gilmanov, T.G. et al., 2007. Partitioning European grassland net ecosystem CO₂ exchange into gross primary productivity and ecosystem respiration using light response function analysis. *Agriculture, Ecosystems & Environment*, 121(1-2): 93-120.
- Gilmanov, T.G. et al., 2005. Integration of CO₂ flux and remotely-sensed data for primary production and ecosystem respiration analyses in the Northern Great Plains: potential for quantitative spatial extrapolation. *Global Ecology and Biogeography*, 14(3): 271-292.
- Gond, V., De Pury, D.G.G., Veroustraete, F., Ceulemans, R., 1999. Seasonal variations in leaf area index, leaf chlorophyll, and water content; scaling-up to estimate fAPAR and carbon balance in a multilayer, multispecies temperate forest. *Tree physiology*, 19(10): 673-679.
- Gouldon, M.L. et al., 2006. An eddy covariance mesonet to measure the effect of forest age on land - atmosphere exchange. *Global Change Biology*, 12(11): 2146-2162.
- Granier, a. et al., 2000. The carbon balance of a young Beech forest. *Functional Ecology*, 14(3): 312-325.
- Gu, L. et al., 2007. Influences of biomass heat and biochemical energy storages on the land surface fluxes and radiative temperature. *Journal of Geophysical Research*, 112(D2): 1-11.
- Gu, L. et al., 2006. Direct and indirect effects of atmospheric conditions and soil moisture on surface energy partitioning revealed by a prolonged drought at a temperate forest site. *Journal of Geophysical Research*, 111(D16): 1-13.
- Hobeichi, S., Abramowitz, G., Evans, J., Ukkola, A., 2018. Derived Optimal Linear Combination Evapotranspiration (DOLCE): a global gridded synthesis ET estimate. *Hydrology and Earth System Sciences*, 22(2): 1317.
- Hollinger, D.Y. et al., 2004. Spatial and temporal variability in forest-atmosphere CO₂ exchange. *Global Change Biology*, 10(10): 1689-1706.
- Hutley, L.B., O'Grady, A.P., Eamus, D., 2000. Evapotranspiration from Eucalypt open-forest savanna of Northern Australia. *Functional Ecology*, 14(2): 183-194.
- Jia, L. et al., 2003. Estimation of sensible heat flux using the Surface Energy Balance System (SEBS) and ATSR measurements. *Physics and Chemistry of the Earth, Parts A/B/C*, 28(1-3): 75-88. DOI:[http://dx.doi.org/10.1016/S1474-7065\(03\)00009-3](http://dx.doi.org/10.1016/S1474-7065(03)00009-3)
- Jiang, C. et al., 2017. Inconsistencies of interannual variability and trends in long-term satellite leaf area index products. *Global change biology*.
- Jiménez, C. et al., 2018. Exploring the merging of the global land evaporation WACMOS-ET products based on local tower measurements. *Hydrology and Earth System Sciences*, 22(8): 4513-4533.
- Jiménez, C. et al., 2011. Global intercomparison of 12 land surface heat flux estimates. *Journal of Geophysical Research*, 116(D2): 1-27.
- Jung, M. et al., 2011. Global patterns of land-atmosphere fluxes of carbon dioxide, latent heat, and sensible heat derived from eddy covariance, satellite, and meteorological observations. *Journal of Geophysical Research*, 116: G00J07.
- Justice, C. et al., 2002. An overview of MODIS Land data processing and product status. *Remote Sensing of Environment*, 83(1-2): 3-15.

- Kala, J. et al., 2014. Influence of leaf area index prescriptions on simulations of heat, moisture, and carbon fluxes. *Journal of Hydrometeorology*, 15(1): 489-503.
- Kalma, J., McVicar, T., McCabe, M., 2008. Estimating Land Surface Evaporation: A Review of Methods Using Remotely Sensed Surface Temperature Data. *Surv Geophys*, 29(4-5): 421-469. DOI:10.1007/s10712-008-9037-z
- Kinne, S. et al., 2013. MAC-v1: A new global aerosol climatology for climate studies. *Journal of Advances in Modeling Earth Systems*, 5(4): 704-740.
- Knohl, A., Schulze, E.-D., Kolle, O., Buchmann, N., 2003. Large carbon uptake by an unmanaged 250-year-old deciduous forest in Central Germany. *Agricultural and Forest Meteorology*, 118(3-4): 151-167.
- Koster, R.D. et al., 2006. GLACE: the global land-atmosphere coupling experiment. Part I: overview. *Journal of Hydrometeorology*, 7(4): 590-610.
- Lafleur, P.M., 2003. Interannual variability in the peatland-atmosphere carbon dioxide exchange at an ombrotrophic bog. *Global Biogeochemical Cycles*, 17(2): 1-14.
- Leng, G. et al., 2013. Modeling the effects of irrigation on land surface fluxes and states over the conterminous United States: Sensitivity to input data and model parameters. *Journal of Geophysical Research: Atmospheres*, 118(17): 9789-9803.
- Leuning, R., Cleugh, H.a., Zegelin, S.J., Hughes, D., 2005. Carbon and water fluxes over a temperate Eucalyptus forest and a tropical wet/dry savanna in Australia: measurements and comparison with MODIS remote sensing estimates. *Agricultural and Forest Meteorology*, 129(3-4): 151-173.
- Liang, S., Wang, K., Zhang, X., Wild, M., 2010. Review on estimation of land surface radiation and energy budgets from ground measurement, remote sensing and model simulations. *IEEE Journal of Selected Topics in Applied Earth Observations and Remote Sensing*, 3(3): 225-240.
- Liu, Y., Liu, R., Chen, J.M., 2012. Retrospective retrieval of long-term consistent global leaf area index (1981–2011) from combined AVHRR and MODIS data. *Journal of Geophysical Research: Biogeosciences*, 117(G4): n/a-n/a. DOI:10.1029/2012JG002084
- Loew, A., Peng, J., Borsche, M., 2016. High-resolution land surface fluxes from satellite and reanalysis data (HOLAPS~ v1. 0): evaluation and uncertainty assessment. *Geoscientific Model Development*, 9: 2499-2532.
- Margulis, S.A., Entekhabi, D., 2001. A Coupled Land Surface–Boundary Layer Model and Its Adjoint. *Journal of Hydrometeorology*, 2(3): 274-296.
- Martens, B. et al., 2017. GLEAM v3: satellite-based land evaporation and root-zone soil moisture. *Geosci. Model Dev.*, 10(5): 1903-1925. DOI:10.5194/gmd-10-1903-2017
- Marx, A., Kunstmann, H., Schüttemeyer, D., Moene, A.F., 2008. Uncertainty analysis for satellite derived sensible heat fluxes and scintillometer measurements over Savannah environment and comparison to mesoscale meteorological simulation results. *Agricultural and Forest Meteorology*, 148(4): 656-667. DOI:<http://dx.doi.org/10.1016/j.agrformet.2007.11.009>
- Mattar, C. et al., 2014. Impacts of the broadband albedo on actual evapotranspiration estimated by S-SEBI model over an agricultural area. *Remote Sensing of Environment*, 147: 23-42. DOI:<https://doi.org/10.1016/j.rse.2014.02.011>

- 613 McCabe, M.F. et al., 2016. The GEWEX LandFlux project: evaluation of model evaporation using tower-based and
614 globally gridded forcing data. *Geoscientific Model Development*, 9(1): 283.
- 615 Meyers, T., 2004. An assessment of storage terms in the surface energy balance of maize and soybean. *Agricultural*
616 *and Forest Meteorology*, 125(1-2): 105-115.
- 617 Michel, D. et al., 2016. The WACMOS-ET project–Part 1: Tower-scale evaluation of four remote-sensing-based
618 evapotranspiration algorithms. *Hydrology and Earth System Sciences*, 20(2): 803.
- 619 Milly, P., Shmakin, A., 2002. Global modeling of land water and energy balances. Part I: The land dynamics (LaD)
620 model. *Journal of Hydrometeorology*, 3(3): 283-299.
- 621 Miralles, D. et al., 2016. The WACMOS-ET project-Part 2: Evaluation of global terrestrial evaporation data sets.
622 *Hydrology and Earth System Sciences*, 20(2): 823-842.
- 623 Miralles, D.G. et al., 2011. Global land-surface evaporation estimated from satellite-based observations. *Hydrol.*
624 *Earth Syst. Sci.*, 15(2): 453-469. DOI:10.5194/hess-15-453-2011
- 625 Mkhabela, M.S. et al., 2009. Comparison of carbon dynamics and water use efficiency following fire and harvesting
626 in Canadian boreal forests. *Agricultural and Forest Meteorology*, 149(5): 783-794.
- 627 Mu, Q., Heinsch, F.A., Zhao, M., Running, S.W., 2007. Development of a global evapotranspiration algorithm
628 based on MODIS and global meteorology data. *Remote sensing of Environment*, 111(4): 519-536.
- 629 Mu, Q., Zhao, M., Running, S.W., 2011. Improvements to a MODIS global terrestrial evapotranspiration algorithm.
630 *Remote Sensing of Environment*, 115(8): 1781-1800.
- 631 Mueller, B. et al., 2013. Benchmark products for land evapotranspiration: LandFlux-EVAL multi-data set synthesis.
632 *Hydrology and Earth System Sciences* 17(10): 3707-3720. DOI:10.5194/hess-17-3707-2013
- 633 Mueller, R.W., Matsoukas, C., Gratzki, A., Behr, H.D., Hollmann, R., 2009. The CM-SAF operational scheme for
634 the satellite based retrieval of solar surface irradiance — A LUT based eigenvector hybrid approach.
635 *Remote Sensing of Environment*, 113(5): 1012-1024. DOI:<http://dx.doi.org/10.1016/j.rse.2009.01.012>
- 636 Muller, J.-P. et al., 2012. The ESA GlobAlbedo Project for mapping the Earth's land surface albedo for 15 Years
637 from European Sensors, *Geophysical Research Abstracts*, pp. 10969.
- 638 Myneni, R.B. et al., 2002. Global products of vegetation leaf area and fraction absorbed PAR from year one of
639 MODIS data. *Remote Sensing of Environment*, 83(1–2): 214-231. DOI:[http://dx.doi.org/10.1016/S0034-](http://dx.doi.org/10.1016/S0034-4257(02)00074-3)
640 [4257\(02\)00074-3](http://dx.doi.org/10.1016/S0034-4257(02)00074-3)
- 641 Nagy, Z. et al., 2007. The carbon budget of semi-arid grassland in a wet and a dry year in Hungary. *Agriculture,*
642 *Ecosystems & Environment*, 121(1–2): 21-29. DOI:<http://dx.doi.org/10.1016/j.agee.2006.12.003>
- 643 Nightingale, J. et al., 2018. Quality Assurance Framework Development Based on Six New ECV Data Products to
644 Enhance User Confidence for Climate Applications. *Remote Sensing*, 10(8): 1254.
- 645 Oki, T., Kanae, S., 2006. Global hydrological cycles and world water resources. *science*, 313(5790): 1068-1072.
- 646 Oleson, K.W. et al., 2003. Assessment of global climate model land surface albedo using MODIS data. *Geophysical*
647 *Research Letters*, 30(8).

- Paulson, C.A., 1970. The Mathematical Representation of Wind Speed and Temperature Profiles in the Unstable Atmospheric Surface Layer. *Journal of Applied Meteorology*, 9(6): 857-861. DOI:10.1175/1520-0450(1970)009<0857:TMROWS>2.0.CO;2
- Peng, J. et al., 2017a. Quality-assured long-term satellite-based leaf area index product. *Global change biology*, 23(12): 5027-5028.
- Peng, J. et al., 2019. The impact of the Madden-Julian Oscillation on hydrological extremes. *Journal of hydrology*, 571: 142-149.
- Peng, J., Liu, Y., Zhao, X., Loew, A., 2013. Estimation of evapotranspiration from MODIS TOA radiances in the Poyang Lake basin, China. *Hydrol. Earth Syst. Sci.*, 17(4): 1431-1444. DOI:10.5194/hess-17-1431-2013
- Peng, J., Loew, A., Chen, X., Ma, Y., Su, Z., 2016. Comparison of satellite-based evapotranspiration estimates over the Tibetan Plateau. *Hydrology and earth system sciences*, 20(8): 3167-3182.
- Peng, J., Loew, A., Merlin, O., Verhoest, N.E., 2017b. A review of spatial downscaling of satellite remotely sensed soil moisture. *Reviews of Geophysics*, 55(2): 341-366.
- Pianosi, F. et al., 2016. Sensitivity analysis of environmental models: A systematic review with practical workflow. *Environmental Modelling & Software*, 79: 214-232.
- Pinty, B. et al., 2006. Simplifying the interaction of land surfaces with radiation for relating remote sensing products to climate models. *Journal of Geophysical Research: Atmospheres*, 111(D2): n/a-n/a. DOI:10.1029/2005JD005952
- Posselt, R., Mueller, R.W., Stöckli, R., Trentmann, J., 2012. Remote sensing of solar surface radiation for climate monitoring — the CM-SAF retrieval in international comparison. *Remote Sensing of Environment*, 118: 186-198.
- Potts, D.R., Mackin, S., Muller, J.P., Fox, N., 2013. Sensor Intercalibration Over Dome C for the ESA GlobAlbedo Project. *Geoscience and Remote Sensing, IEEE Transactions on*, 51(3): 1139-1146. DOI:10.1109/TGRS.2012.2217749
- Priestley, C., Taylor, R., 1972. On the assessment of surface heat flux and evaporation using large-scale parameters. *Monthly weather review*, 100(2): 81-92.
- Rebmann, C. et al., 2010. Treatment and assessment of the CO₂-exchange at a complex forest site in Thuringia, Germany. *Agricultural and Forest Meteorology*, 150(5): 684-691.
- Richard, W. et al., 2018. Evapotranspiration simulations in ISIMIP2a—Evaluation of spatio-temporal characteristics with a comprehensive ensemble of independent datasets. *Environmental Research Letters*, 13(7): 075001.
- Richards, L.A., 1931. Capillary conduction of liquids through porous mediums. *Journal of Applied Physics*, 1(5): 318-333. DOI:doi:<http://dx.doi.org/10.1063/1.1745010>
- Roads, J., Betts, A., 2000. NCEP–NCAR and ECMWF Reanalysis Surface Water and Energy Budgets for the Mississippi River Basin. *Journal of Hydrometeorology*, 1(1): 88-94. DOI:10.1175/1525-7541(2000)001<0088:NNAERS>2.0.CO;2
- Saltelli, A., 1999. Sensitivity analysis: Could better methods be used? *Journal of Geophysical Research: Atmospheres*, 104(D3): 3789-3793.

- 685 Saltelli, A. et al., 2010. Variance based sensitivity analysis of model output. Design and estimator for the total
686 sensitivity index. *Computer Physics Communications*, 181(2): 259-270.
- 687 Scherer-Lorenzen, M., Schulze, E., Don, A., Schumacher, J., Weller, E., 2007. Exploring the functional significance
688 of forest diversity: A new long-term experiment with temperate tree species (BIOTREE). *Perspectives in*
689 *Plant Ecology, Evolution and Systematics*, 9(2): 53-70.
- 690 Seneviratne, S.I., Lüthi, D., Litschi, M., Schär, C., 2006. Land-atmosphere coupling and climate change in Europe.
691 *Nature*, 443(7108): 205.
- 692 Siemann, A.L., Chaney, N., Wood, E.F., 2018. Development and Validation of a Long Term, Global, Terrestrial
693 Sensible Heat Flux Dataset. *Journal of Climate*, 0(0): null. DOI:10.1175/jcli-d-17-0732.1
- 694 Song, R., Muller, J.-P., Kharbouche, S., Woodgate, W., 2019. Intercomparison of Surface Albedo Retrievals from
695 MISR, MODIS, CGLS Using Tower and Upscaled Tower Measurements. *Remote Sensing*, 11(6): 644.
- 696 Stroeve, J. et al., 2005. Accuracy assessment of the MODIS 16-day albedo product for snow: comparisons with
697 Greenland in situ measurements. *Remote Sensing of Environment*, 94(1): 46-60.
- 698 Su, Z., 2002. The Surface Energy Balance System (SEBS) for estimation of turbulent heat fluxes. *Hydrol. Earth*
699 *Syst. Sci.*, 6(1): 85-100. DOI:10.5194/hess-6-85-2002
- 700 Suni, T. et al., 2015. The significance of land-atmosphere interactions in the Earth system—iLEAPS achievements
701 and perspectives. *Anthropocene*, 12: 69-84. DOI:<https://doi.org/10.1016/j.ancene.2015.12.001>
- 702 Talsma, C. et al., 2018. Sensitivity of Evapotranspiration Components in Remote Sensing-Based Models. *Remote*
703 *Sensing*, 10(10): 1601.
- 704 Tang, R., Li, Z.-L., Chen, K.-S., 2011a. Validating MODIS-derived land surface evapotranspiration with in situ
705 measurements at two AmeriFlux sites in a semiarid region. *Journal of Geophysical Research*, 116(D4):
706 D04106.
- 707 Tang, R. et al., 2011b. An intercomparison of three remote sensing-based energy balance models using Large
708 Aperture Scintillometer measurements over a wheat-corn production region. *Remote Sensing of*
709 *Environment*, 115(12): 3187-3202. DOI:<http://dx.doi.org/10.1016/j.rse.2011.07.004>
- 710 Taylor, K.E., 2001. Summarizing multiple aspects of model performance in a single diagram. *Journal of*
711 *Geophysical Research*, 106(D7): 7183-7192.
- 712 Tedeschi, V. et al., 2006. Soil respiration in a Mediterranean oak forest at different developmental stages after
713 coppicing. *Global Change Biology*, 12(1): 110-121.
- 714 Trenberth, K.E., Smith, L., Qian, T., Dai, A., Fasullo, J., 2007. Estimates of the global water budget and its annual
715 cycle using observational and model data. *Journal of Hydrometeorology*, 8(4): 758-769.
- 716 Twine, T.E. et al., 2000. Correcting eddy-covariance flux underestimates over a grassland. *Agricultural and Forest*
717 *Meteorology*, 103(3): 279-300.
- 718 Verma, S.B. et al., 2005. Annual carbon dioxide exchange in irrigated and rainfed maize-based agroecosystems.
719 *Agricultural and Forest Meteorology*, 131(1-2): 77-96.
- 720 Vinukollu, R.K., Wood, E.F., Ferguson, C.R., Fisher, J.B., 2011. Global estimates of evapotranspiration for climate
721 studies using multi-sensor remote sensing data: Evaluation of three process-based approaches. *Remote*
722 *Sensing of Environment*, 115(3): 801-823. DOI:<http://dx.doi.org/10.1016/j.rse.2010.11.006>

- Voßbeck, M. et al., 2010. An inverse radiative transfer model of the vegetation canopy based on automatic differentiation. *Inverse Problems*, 26(9): 095003.
- Wang, D. et al., 2015. Estimating daily mean land surface albedo from MODIS data. *Journal of Geophysical Research: Atmospheres*, 120(10): 4825-4841.
- Wang, D., Liang, S., Zhou, Y., He, T., Yu, Y., 2016. A new method for retrieving daily land surface albedo from VIIRS data. *IEEE Transactions on Geoscience and Remote Sensing*, 55(3): 1765-1775.
- Wang, K., Dickinson, R.E., 2012. A review of global terrestrial evapotranspiration: Observation, modeling, climatology, and climatic variability. *Reviews of Geophysics*, 50(2). DOI:10.1029/2011RG000373
- Wang, K., Wang, P., Li, Z., Cribb, M., Sparrow, M., 2007. A simple method to estimate actual evapotranspiration from a combination of net radiation, vegetation index, and temperature. *Journal of Geophysical Research: Atmospheres*, 112(D15).
- Wang, Y., Li, X., Tang, S., 2013. Validation of the SEBS-derived sensible heat for FY3A/VIRR and TERRA/MODIS over an alpine grass region using LAS measurements. *International Journal of Applied Earth Observation and Geoinformation*, 23: 226-233. DOI:<http://dx.doi.org/10.1016/j.jag.2012.09.005>
- Wang, Z. et al., 2004. Using MODIS BRDF and albedo data to evaluate global model land surface albedo. *Journal of Hydrometeorology*, 5(1): 3-14.
- Wild, M. et al., 2015. The energy balance over land and oceans: an assessment based on direct observations and CMIP5 climate models. *Climate Dynamics*, 44(11-12): 3393-3429.
- Wohlfahrt, G. et al., 2008. Seasonal and inter-annual variability of the net ecosystem CO₂ exchange of a temperate mountain grassland: Effects of weather and management. *Journal of Geophysical Research*, 113(D8).
- Yang, F. et al., 2008. Assessing the representativeness of the AmeriFlux network using MODIS and GOES data. *Journal of Geophysical Research*, 113(G4): G04036.
- Yao, Y. et al., 2017. Improving global terrestrial evapotranspiration estimation using support vector machine by integrating three process-based algorithms. *Agricultural and forest meteorology*, 242: 55-74.
- Yuan, H., Dai, Y., Xiao, Z., Ji, D., Shangguan, W., 2011. Reprocessing the MODIS Leaf Area Index products for land surface and climate modelling. *Remote Sensing of Environment*, 115(5): 1171-1187.
- Zhang, K., Kimball, J.S., Nemani, R.R., Running, S.W., 2010. A continuous satellite-derived global record of land surface evapotranspiration from 1983 to 2006. *Water Resources Research*, 46(9).
- Zhang, K., Kimball, J.S., Running, S.W., 2016. A review of remote sensing based actual evapotranspiration estimation. *Wiley Interdisciplinary Reviews: Water*, 3(6): 834-853.
- Zhang, X., Berhane, T., Seielstad, G., 2008. Comparison of Landsat and MODIS Estimates of Heat Fluxes: Effect of Surface Heterogeneity, IGARSS 2008 - 2008 IEEE International Geoscience and Remote Sensing Symposium. IEEE, pp. 759 - 762.
- Zhu, Z. et al., 2016. Greening of the Earth and its drivers. *Nature climate change*, 6(8): 791-795.
- Zhuang, Q., Wu, B., Yan, N., Zhu, W., Xing, Q., 2016. A method for sensible heat flux model parameterization based on radiometric surface temperature and environmental factors without involving the parameter

KB-1. International Journal of Applied Earth Observation and Geoinformation, 47: 50-59.
DOI:<http://dx.doi.org/10.1016/j.jag.2015.11.015>

Influences of leaf area index and albedo on estimating energy fluxes with HOLAPS framework

Jian Peng^{1,2,3*}, Said Kharbouche ⁴, Jan Peter-Muller ⁴, Olaf Danne ⁵, Simon Blessing ⁶, Ralf Giering ⁶, Nadine Gobron ⁷, Ralf Ludwig ², Benjamin Müller ², Guoyong Leng ⁸, Thomas Lees ¹, Simon Dadson ¹

¹ School of Geography and the Environment, University of Oxford, OX1 3QY Oxford, UK;

² Department of Geography, University of Munich (LMU), 80333 Munich, Germany;

³ Max Planck Institute for Meteorology, 20146 Hamburg, Germany;

⁴ Department of Space and Climate Physics, University College London, Holmbury St Mary, UK;

⁵ Brockmann Consult GmbH, Max-Planck Str.2, 21502 Geesthacht, Germany;

⁶ FastOpt, Hamburg, Germany;

⁷ Directorate for Sustainable Resources, European Commission, Joint Research Centre, Ispra, Italy;

⁸ Environmental Change Institute, University of Oxford, OX1 3QY Oxford, UK;

* Author to whom correspondence should be addressed; E-Mail: jian.peng@ouce.ox.ac.uk;

Abstract

The High resOlution Land Atmosphere surface Parameters from Space (HOLAPS) programme provides a modeling system to maximize the use of satellite-based products and ensure internally consistent estimation of surface water and energy fluxes. Leaf area index (LAI) and land surface albedo are two key parameters for estimation of latent and sensible heat fluxes with HOLAPS. Thus, to facilitate the generation of long-term high accuracy latent and sensible heat fluxes, high quality global long-term LAI and land surface albedo datasets are essential. The Quality Assurance for Essential Climate Variables (QA4ECV) project released quality-assured long-term LAI and albedo datasets with traceable and reliable uncertainty information provided in the dataset. Taking MODIS-BNU-LAI and MODIS albedo as reference, different global long-term LAI and albedo datasets including GlobAlbedo, QA4ECV and GLOBMAP were investigated for estimation of latent/sensible heat fluxes with HOLAPS in this study. The results show that all albedo datasets show similar accuracy for estimation of latent and sensible heat fluxes when validated against FLUXNET observations. The QA4ECV LAI leads to worse latent heat flux estimation due to its use of effective LAI rather than green leaf LAI. Sensitivity analysis also shows that the HOLAPS estimated latent heat flux (LE) is more sensitive to uncertainty in LAI than land surface albedo. Overall, the combined use of QA4ECV albedo and GLOBMAP LAI is suggested for estimation of latent/sensible heat fluxes with HOLAPS. The root mean square differences (RMSD) between estimations and FLUXNET measurements are 54 (30) W/m² for hourly (monthly) latent heat flux, and 80.5 (24.5) W/m² for sensible heat flux, which are comparable to estimates with MODIS and other reported studies.

1. The newly developed global long-term QA4ECV albedo and LAI datasets were applied for latent and sensible heat fluxes estimation
2. The QA4ECV LAI leads to worse latent heat flux estimation due to its use of effective LAI rather than green leaf LAI
3. The combined use of QA4ECV albedo and GLOBMAP LAI was suggested for latent and sensible heat fluxes estimation based on HOLAPS

Declaration of interests

☒ The authors declare that they have no known competing financial interests or personal relationships that could have appeared to influence the work reported in this paper.

☐ The authors declare the following financial interests/personal relationships which may be considered as potential competing interests:

819
820
821
822
823

Journal Pre-proofs